

---

## Report 5. Homogeneous and coaxially loaded cylindrical resonators made of frequency dependent lossy material

---

BSc. Malgorzata Warecka  
September 1, 2017



This work was supported by project EDISON - Electromagnetic Design of flexibleSensOrs, *The „EDISON” project is carried out within the TEAM-TECH programme programme of the Foundation for Polish Science co-financed by the European Union under the European Regional Development Fund.*

Revision	Date	Author(s)	Description
1.0	1.09.2017	M. Warecka	created
1.0	1.09.2017	P. Kowalczyk	checked

## 1 Introduction

The aim of the report is to show the results of analysis for two closed structures: homogeneous and coaxially loaded cylindrical resonators presented in the Fig. 1.

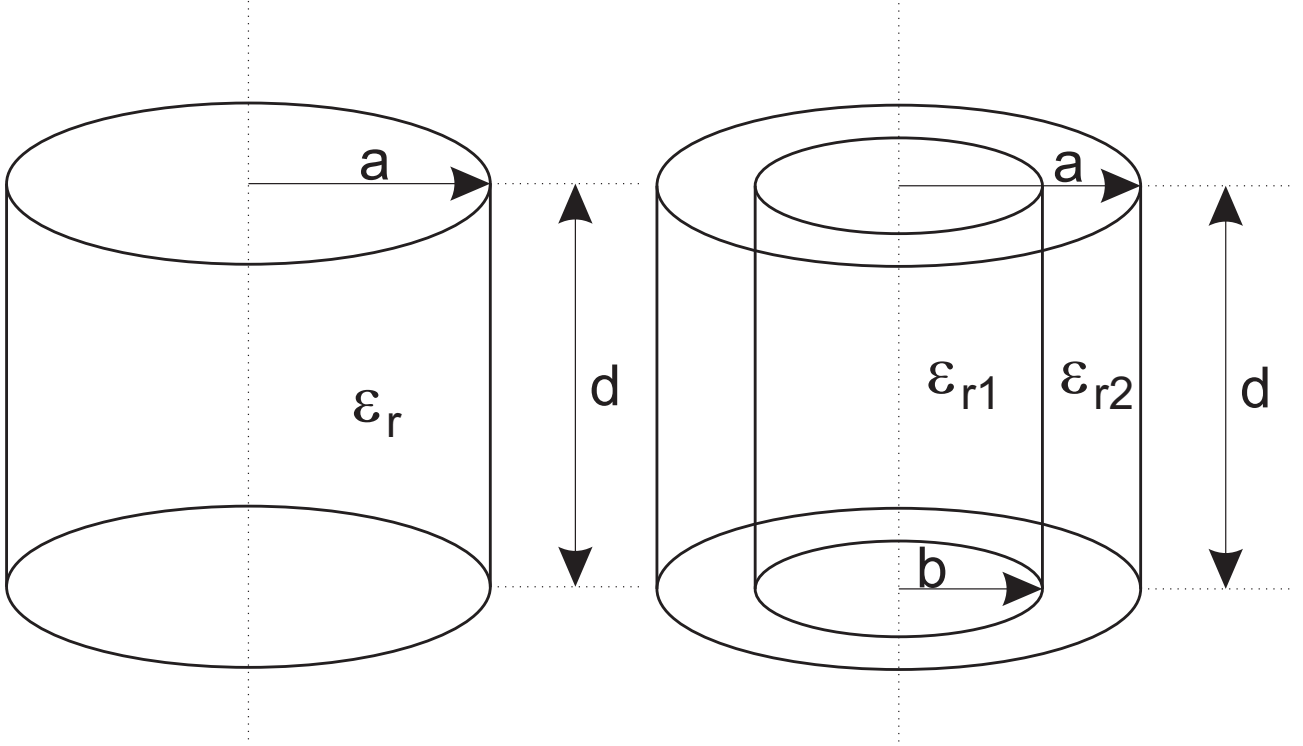


Figure 1: Homogeneous (left) and coaxially loaded (right) cylindrical resonators.

The first considered cylindrical resonator is fully filled with lossy material. The second (coaxially loaded) resonator can be divided into two regions. The first region is a lossy layer and the second one is a vacuum. The permittivity of lossy material can be expressed as  $\epsilon_r = \epsilon'_r - j \frac{\sigma}{\omega \epsilon_0}$  where  $\sigma$  is the conductivity of the material,  $\omega$  is the angular frequency and  $\epsilon_0$  is the permittivity of the vacuum. Results of the analysis are presented in the next sections. For all calculations constants have value  $c = 2.99792458 \cdot 10^8 \frac{m}{s}$ ,  $\mu_0 = 4\pi 10^{-7} \frac{H}{m}$  and  $\epsilon_0 = \frac{1}{c^2 \mu_0}$ . The tolerance of the found frequencies (using root finding algorithm [1]) is  $10^{-10}$  [GHz].

## 2 Problem formulation

The electric and magnetic fields for cylindrical resonators have the following form (directly from Maxwell's equations):

$$\widehat{E}_z = E_z(\rho) \cos(m\phi) \cos\left(\frac{l\pi}{d} z\right) \quad (1)$$

$$\widehat{E}_\rho = E_\rho(\rho) \cos(m\phi) \sin\left(\frac{l\pi}{d} z\right) \quad (2)$$

$$\widehat{E}_\phi = E_\phi(\rho) \sin(m\phi) \sin\left(\frac{l\pi}{d} z\right) \quad (3)$$

$$\widehat{H}_z = H_z(\rho) \sin(m\phi) \sin\left(\frac{l\pi}{d} z\right) \quad (4)$$

$$\widehat{H}_\rho = H_\rho(\rho) \sin(m\phi) \cos\left(\frac{l\pi}{d}z\right) \quad (5)$$

$$\widehat{H}_\phi = H_\phi(\rho) \cos(m\phi) \cos\left(\frac{l\pi}{d}z\right) \quad (6)$$

where m, n and l refer to the field variation with respect to  $\phi$ ,  $\rho$  and  $z$ , respectively. The boundary conditions can be written as:

$$\frac{\partial \widehat{E}_z(\rho, \phi, d)}{\partial z} = 0 \quad (7)$$

$$\frac{\partial \widehat{E}_z(\rho, \phi, 0)}{\partial z} = 0 \quad (8)$$

$$E_\phi(\rho, \phi, d) = 0 \quad (9)$$

$$E_\phi(\rho, \phi, 0) = 0 \quad (10)$$

$$E_\phi(a, \phi, z) = 0 \quad (11)$$

$$E_z(a, \phi, z) = 0 \quad (12)$$

## 2.1 Homogeneous cylindrical resonators

The equations for the homogeneous resonator can be separated due to the symmetry of the structure. Direct consequences of the separation of equations are transverse magnetic and electric modes in the resonator.

For  $TM_{mnl}$  modes, the fields can be expressed as:

$$E_\rho(\rho) = -\frac{j l \pi}{d \kappa} A J'_m(\kappa \rho) \quad (13)$$

$$E_\phi(\rho) = \frac{l \pi m}{d \kappa^2 \rho} A J_m(\kappa \rho) \quad (14)$$

$$E_z(\rho) = A J_m(\kappa \rho) \quad (15)$$

$$H_\rho(\rho) = -\frac{j \omega \varepsilon m}{\kappa^2 \rho} A J_m(\kappa \rho) \quad (16)$$

$$H_\phi(\rho) = -\frac{\omega \varepsilon m}{\kappa} A J_m(\kappa \rho) \quad (17)$$

$$H_z(\rho) = 0 \quad (18)$$

and for  $TE_{mnl}$  modes :

$$E_\rho(\rho) = \frac{\omega \mu m}{\rho \kappa^2} A J_m(\kappa \rho) \quad (19)$$

$$E_\phi(\rho) = \frac{\omega \mu}{\kappa} A J'_m(\kappa \rho) \quad (20)$$

$$E_z(\rho) = 0 \quad (21)$$

$$H_\rho(\rho) = -\frac{j l \pi}{d \kappa} A J'_m(\kappa \rho) \quad (22)$$

$$H_\phi(\rho) = \frac{j l \pi m}{d \kappa^2 \rho} A J_m(\kappa \rho) \quad (23)$$

$$H_z(\rho) = -j A J_m(\kappa \rho) \quad (24)$$

where  $\kappa^2 = \left(\frac{2\pi f}{c}\right)^2 \varepsilon_r + \left(\frac{j l \pi}{d}\right)^2$ ,  $J_m$  is the Bessel function,  $Y_m$  is the Neumann function. The usage of the boundary conditions reduces the problem to finding zeros of the following expression:

- for TM modes

$$J_m(\kappa a) = 0 \quad (25)$$

- for TE modes

$$J'_m(\kappa a) = 0 \quad (26)$$

## 2.2 Coaxially loaded cylindrical resonator

If we consider the coaxially loaded cylindrical resonator, then the fields can be expressed as:

$$E_z^I(\rho) = A^I J_m(\kappa_1 \rho) \quad (27)$$

$$E_\phi^I(\rho) = \frac{l\pi m}{d\kappa_1^2 \rho} A^I J_m(\kappa_1 \rho) + \frac{j\omega\mu_1}{\kappa_1} C^I J'_m(\kappa_1 \rho) \quad (28)$$

$$H_z^I(\rho) = C^I J_m(\kappa_1 \rho) \quad (29)$$

$$H_\phi^I(\rho) = \frac{l\pi m}{d\kappa_1^2 \rho} C^I J_m(\kappa_1 \rho) - \frac{j\omega\varepsilon_1}{\kappa_1} A^I J'_m(\kappa_1 \rho) \quad (30)$$

in the first region and

$$E_z^{II}(\rho) = A^{II} J_m(\kappa_2 \rho) + B^{II} Y_m(\kappa_2 \rho) \quad (31)$$

$$E_\phi^{II}(\rho) = \frac{l\pi m}{d\kappa_2^2 \rho} A^{II} J_m(\kappa_2 \rho) + \frac{l\pi m}{d\kappa_2^2 \rho} B^{II} Y_m(\kappa_2 \rho) + \frac{j\omega\mu_2}{\kappa_2} C^{II} J'_m(\kappa_2 \rho) + \frac{j\omega\mu_2}{\kappa_2} D^{II} Y'_m(\kappa_2 \rho) \quad (32)$$

$$H_z^{II}(\rho) = C^{II} J_m(\kappa_2 \rho) + D^{II} Y_m(\kappa_2 \rho) \quad (33)$$

$$H_\phi^{II}(\rho) = \frac{l\pi m}{d\kappa_2^2 \rho} C^{II} J_m(\kappa_2 \rho) + \frac{l\pi m}{d\kappa_2^2 \rho} D^{II} Y_m(\kappa_2 \rho) + \frac{j\omega\mu_2}{\kappa_2} A^{II} J'_m(\kappa_2 \rho) + \frac{j\omega\mu_2}{\kappa_2} B^{II} Y'_m(\kappa_2 \rho) \quad (34)$$

in the second region. The resonance frequencies for this structure can be found also from boundary conditions (7-12) and continuity of the fields at the connection of the regions, by finding the roots of the following determinant:

$$\begin{vmatrix} J_m(\kappa_1 a) & 0 & -J_m(\kappa_2 a) & -Y_m(\kappa_2 a) & 0 & 0 \\ 0 & J_m(\kappa_1 a) & 0 & 0 & -J_m(\kappa_2 a) & -Y_m(\kappa_2 a) \\ -\frac{j\omega\varepsilon_1}{\kappa_1} J'_m(\kappa_1 a) & \frac{l\pi m}{da\kappa_1^2} J_m(\kappa_1 a) & \frac{j\omega\varepsilon_2}{\kappa_2} J'_m(\kappa_2 a) & \frac{j\omega\varepsilon_2}{\kappa_2} Y'_m(\kappa_2 a) & -\frac{l\pi m}{da\kappa_2^2} J_m(\kappa_2 a) & -\frac{l\pi m}{da\kappa_2^2} Y_m(\kappa_2 a) \\ \frac{l\pi m}{da\kappa_1^2} J_m(\kappa_1 a) & \frac{j\omega\mu_1}{\kappa_1} J'_m(\kappa_1 a) & -\frac{l\pi m}{da\kappa_2^2} J_m(\kappa_2 a) & -\frac{l\pi m}{da\kappa_2^2} Y_m(\kappa_2 a) & -\frac{j\omega\mu_2}{\kappa_2} J'_m(\kappa_2 a) & -\frac{j\omega\mu_2}{\kappa_2} Y'_m(\kappa_2 a) \\ 0 & 0 & \frac{l\pi m}{db\kappa_2^2} J_m(\kappa_2 b) & \frac{l\pi m}{db\kappa_2^2} Y_m(\kappa_2 b) & \frac{j\omega\mu_2}{\kappa_2} J'_m(\kappa_2 b) & \frac{j\omega\mu_2}{\kappa_2} Y'_m(\kappa_2 b) \\ 0 & 0 & J_m(\kappa_2 b) & Y_m(\kappa_2 b) & 0 & 0 \end{vmatrix} = 0 \quad (35)$$

## 3 Results

### 3.1 Homogeneous cylindrical resonator

This section presents results for transverse magnetic and transverse electric modes in the homogeneous cylindrical resonator. The geometrical dimensions used in the analysis are  $d = 10\sqrt{2}mm$  and  $a = 10mm$  (see Fig.1) and the relative permittivity is  $\varepsilon_r = 10$ . The analysed modes are described in the table 1. In the first step the analysis is performed for  $\sigma = 0$  and the results are presented in the table 2. The complex resonance frequencies as a function of conductivity (in the range 0 to 100 S/m) are presented in the Fig. 2-4 and shown in the table 2. The initial mesh step in the global root finding algorithm [1] is set to 0.01 [GHz]. In table 4 Q factor of the resonator as a function of  $\sigma$  is presented.

### 3.2 Coaxially loaded cylindrical resonator

This section demonstrates the results for modes in a coaxially loaded cylindrical resonator. The geometrical dimensions used in the analysis are  $d = 10\sqrt{2}mm$ ,  $a = 6.35mm$  and  $b = 10mm$  (see Fig.1) and the and the relative permittivities are  $\varepsilon_{r2} = 1$  and  $\varepsilon'_{r1} = 10$ . The analysed modes are described in the table 5. In the first step the analysis is performed for  $\sigma = 0$  and the results are presented in the table 2. The complex resonance frequencies as a function of conductivity (in the range 0 to 50 S/m) are presented in the Fig. 5-7 collected in the table 3.2. The results are confronted with the results for the coaxially loaded resonator with perfect electric conductor (see table 8). The initial mesh step in the global root finding algorithm [1] is set to 0.01 [GHz]. In table 7 Q factor of the resonator as a function of  $\sigma$  is presented.

Table 2: Modes presented in Fig.2-4.

mode	color in figure	line style
$TE_{011}$	red	solid
$TE_{012}$	green	solid
$TE_{111}$	black	solid
$TE_{112}$	cyan	solid
$TE_{121}$	magenta	solid
$TE_{211}$	yellow	solid
$TE_{212}$	blue	dotted
$TE_{311}$	red	dotted
$TE_{411}$	green	dotted
$TM_{010}$	black	dotted
$TM_{011}$	cyan	dotted
$TM_{012}$	magenta	dotted
$TM_{020}$	yellow	dotted
$TM_{021}$	blue	dashed
$TM_{110}$	red	dashed
$TM_{111}$	green	dashed
$TM_{112}$	black	dashed
$TM_{210}$	cyan	dashed
$TM_{211}$	magenta	dashed
$TM_{310}$	yellow	dashed

Table 3: The resonance frequencies for  $\sigma = 0$ 

	homogeneous	partially loaded	
	$\epsilon_{r2} = 10$	$\epsilon_{r2} = 1$	
$TM_{010}$	3.628477324	3.883856934	$TM_{010}$
$TE_{111}$	4.353381158	6.088975322	$HE_{111}$
$TM_{011}$	4.939664708	8.193372828	$TM_{011}$
$TE_{211}$	5.698345714	9.884743615	$HE_{211}$
$TM_{110}$	5.781399895	6.618765916	$TM_{110}$
$TM_{111}$	6.682740791	9.884743615	$EH_{111}$
$TE_{011}$	6.682740791	7.575026719	$HE_{011}$
$TE_{311}$	7.170490584	12.308462125	$HE_{311}$
$TE_{112}$	7.256393506	8.439295609	$HE_{112}$
$TM_{012}$	7.622572179	10.941790074	$TM_{012}$
$TM_{210}$	7.748790347	9.389886432	$TM_{210}$
$TE_{212}$	8.134768778	10.796266012	$HE_{212}$
$TM_{020}$	8.328869505	10.120293653	$TM_{020}$
$TM_{211}$	8.442641268	12.403656676	$EH_{211}$
$TE_{411}$	8.695267456	15.220919382	$HE_{411}$
$TE_{121}$	8.714608766	11.393804922	$HE_{121}$
$TE_{012}$	8.852250769	9.8095604466	$HE_{012}$
$TM_{112}$	8.852250769	12.101986836	$EH_{112}$
$TM_{021}$	8.978001279	12.187616669	$TM_{021}$
$TM_{310}$	9.626591289	12.204096657	$TM_{310}$

Table 4: The resonance frequencies of the homogeneous resonator as a function of the conductivity.

$\sigma$	0.01	0.05
$TM_{011}$	4.939656531 + 0.008987551i	4.939460297 + 0.044937758i
$TM_{011}$	4.939656531 + 0.008987551i	4.939460297 + 0.044937758i
$TM_{021}$	8.977996780 + 0.008987551i	8.977888814 + 0.044937758i
$TM_{021}$	8.977996780 + 0.008987551i	8.977888814 + 0.044937758i
$TM_{010}$	3.628466193 + 0.008987551i	3.628199042 + 0.044937758i
$TM_{010}$	3.628466193 + 0.008987551i	3.628199042 + 0.044937758i
$TM_{020}$	8.328864655 + 0.008987551i	8.328748275 + 0.044937758i
$TM_{020}$	8.328864655 + 0.008987551i	8.328748275 + 0.044937758i
$TM_{110}$	5.781392909 + 0.008987551i	5.781225245 + 0.044937758i
$TM_{110}$	5.781392909 + 0.008987551i	5.781225245 + 0.044937758i
$TM_{210}$	7.748785135 + 0.008987551i	7.748660042 + 0.044937758i
$TM_{210}$	7.748785135 + 0.008987551i	7.748660042 + 0.044937758i
$TM_{310}$	9.626587093 + 0.008987551i	9.626486401 + 0.044937758i
$TM_{310}$	9.626587093 + 0.008987551i	9.626486401 + 0.044937758i
$TM_{111}$	6.682734747 + 0.008987551i	6.682589698 + 0.044937758i
$TM_{111}$	6.682734747 + 0.008987551i	6.682589698 + 0.044937758i
$TM_{211}$	8.442636484 + 0.008987551i	8.442521672 + 0.044937758i
$TM_{211}$	8.442636484 + 0.008987551i	8.442521672 + 0.044937758i
$TM_{112}$	8.852246206 + 0.008987551i	8.852136707 + 0.044937758i
$TM_{112}$	8.852246206 + 0.008987551i	8.852136707 + 0.044937758i
$TE_{011}$	6.682734747 + 0.008987551i	6.682589698 + 0.044937758i
$TE_{011}$	6.682734747 + 0.008987551i	6.682589698 + 0.044937758i
$TE_{012}$	8.852246206 + 0.008987551i	8.852136707 + 0.044937758i
$TE_{012}$	8.852246206 + 0.008987551i	8.852136707 + 0.044937758i
$TM_{012}$	7.622566880 + 0.008987551i	7.622439716 + 0.044937758i
$TM_{012}$	7.622566880 + 0.008987551i	7.622439716 + 0.044937758i
$TE_{111}$	4.353371881 + 0.008987551i	4.353149217 + 0.044937758i
$TE_{111}$	4.353371881 + 0.008987551i	4.353149217 + 0.044937758i
$TE_{121}$	8.714604131 + 0.008987551i	8.714492902 + 0.044937758i
$TE_{121}$	8.714604131 + 0.008987551i	8.714492902 + 0.044937758i
$TE_{211}$	5.698338626 + 0.008987551i	5.698168519 + 0.044937758i
$TE_{211}$	5.698338626 + 0.008987551i	5.698168519 + 0.044937758i
$TE_{112}$	7.256387940 + 0.008987551i	7.256254358 + 0.044937758i
$TE_{112}$	7.256387940 + 0.008987551i	7.256254358 + 0.044937758i
$TE_{311}$	7.170484951 + 0.008987551i	7.170349769 + 0.044937758i
$TE_{311}$	7.170484951 + 0.008987551i	7.170349769 + 0.044937758i
$TE_{212}$	8.134763813 + 0.008987551i	8.134644655 + 0.044937758i
$TE_{212}$	8.134763813 + 0.008987551i	8.134644655 + 0.044937758i
$TE_{411}$	8.695262811 + 0.008987551i	8.695151335 + 0.044937758i
$TE_{411}$	8.695262811 + 0.008987551i	8.695151335 + 0.044937758i

$\sigma$	0.1	0.5
$TM_{011}$	4.938847013 + 0.089875517i	4.919181559 + 0.449377589i
$TM_{011}$	4.938847013 + 0.089875517i	4.919181559 + 0.449377589i
$TM_{021}$	8.977551412 + 0.089875517i	8.966747835 + 0.449377589i
$TM_{021}$	8.977551412 + 0.089875517i	8.966747835 + 0.449377589i
$TM_{010}$	3.627364068 + 0.089875517i	3.600542664 + 0.449377589i
$TM_{010}$	3.627364068 + 0.089875517i	3.600542664 + 0.449377589i
$TM_{020}$	8.328384574 + 0.0898755178i	8.31673776 + 0.449377589i
$TM_{020}$	8.328384574 + 0.0898755178i	8.31673776 + 0.449377589i
$TM_{110}$	5.780701266 + 0.0898755178i	5.76390878 + 0.449377589i
$TM_{110}$	5.780701266 + 0.0898755178i	5.76390878 + 0.449377589i
$TM_{210}$	7.748269112 + 0.0898755178i	7.73574893 + 0.449377589i
$TM_{210}$	7.748269112 + 0.0898755178i	7.73574893 + 0.449377589i
$TM_{310}$	9.626171733 + 0.089875517i	9.616096902 + 0.449377589i
$TM_{310}$	9.626171733 + 0.089875517i	9.616096902 + 0.449377589i
$TM_{111}$	6.682136400 + 0.089875517i	6.667614585 + 0.449377589i
$TM_{111}$	6.682136400 + 0.089875517i	6.667614585 + 0.449377589i
$TM_{211}$	8.442162873 + 0.089875517i	8.430673245 + 0.449377589i
$TM_{211}$	8.442162873 + 0.089875517i	8.430673245 + 0.449377589i
$TM_{112}$	8.851794511 + 0.089875517i	8.840837260 + 0.449377589i
$TM_{112}$	8.851794511 + 0.089875517i	8.840837260 + 0.449377589i
$TE_{011}$	6.682136400 + 0.089875517i	6.667614585 + 0.449377589i
$TE_{011}$	6.682136400 + 0.089875517i	6.667614585 + 0.449377589i
$TE_{012}$	8.851794511 + 0.089875517i	8.840837260 + 0.449377589i
$TE_{012}$	8.851794511 + 0.089875517i	8.840837260 + 0.449377589i
$TM_{012}$	7.622042313 + 0.089875517i	7.609314450 + 0.449377589i
$TM_{012}$	7.622042313 + 0.089875517i	7.609314450 + 0.449377589i
$TE_{111}$	4.352453320 + 0.089875517i	4.330125551 + 0.449377589i
$TE_{111}$	4.352453320 + 0.089875517i	4.330125551 + 0.449377589i
$TE_{121}$	8.714145301 + 0.089875517i	8.703014749 + 0.449377589i
$TE_{121}$	8.714145301 + 0.089875517i	8.703014749 + 0.449377589i
$TE_{211}$	5.697636902 + 0.089875517i	5.6805988821 + 0.44937758i
$TE_{211}$	5.697636902 + 0.089875517i	5.6805988822 + 0.44937758i
$TE_{112}$	7.255836899 + 0.089875517i	7.2424654984 + 0.44937758i
$TE_{112}$	7.255836899 + 0.089875517i	7.2424654984 + 0.44937758i
$TE_{311}$	7.169927308 + 0.089875517i	7.1563953915 + 0.44937758i
$TE_{311}$	7.169927308 + 0.089875517i	7.1563953915 + 0.44937758i
$TE_{212}$	8.134272276 + 0.089875517i	8.1223471277 + 0.44937758i
$TE_{212}$	8.134272276 + 0.089875517i	8.1223471277 + 0.44937758i
$TE_{411}$	8.694802961 + 0.089875517i	8.6836476164 + 0.44937758i
$TE_{411}$	8.694802961 + 0.089875517i	8.6836476164 + 0.44937758i

$\sigma$	1	5
$TM_{011}$	4.857213867 + 0.898755178i	2.050918244 + 4.493775893i
$TM_{011}$	4.857213867 + 0.898755178i	2.050918244 + 4.493775893i
$TM_{021}$	8.932902445 + 0.898755178i	7.772418232 + 4.493775893i
$TM_{021}$	8.932902445 + 0.898755178i	7.772418232 + 4.493775893i
$TM_{010}$	3.515407063 + 0.898755178i	1.842705527i
$TM_{010}$	3.515407063 + 0.898755178i	7.144846260i
$TM_{020}$	8.280235887 + 0.898755178i	7.012563400 + 4.493775893i
$TM_{020}$	8.280235887 + 0.898755178i	7.012563400 + 4.493775893i
$TM_{110}$	5.711114066 + 0.898755178i	3.637384082 + 4.493775893i
$TM_{110}$	5.711114066 + 0.898755178i	3.637384082 + 4.493775893i
$TM_{210}$	7.696492121 + 0.898755178i	6.312664260 + 4.493775893i
$TM_{210}$	7.696492121 + 0.898755178i	6.312664260 + 4.493775893i
$TM_{310}$	9.584544797 + 0.898755178i	8.513356451 + 4.493775893i
$TM_{310}$	9.584544797 + 0.898755178i	8.513356451 + 4.493775893i
$TM_{111}$	6.622028662 + 0.898755178i	4.946210943 + 4.493775893i
$TM_{111}$	6.622028662 + 0.898755178i	4.946210943 + 4.493775893i
$TM_{211}$	8.394666801 + 0.898755178i	7.147319064 + 4.493775893i
$TM_{211}$	8.394666801 + 0.898755178i	7.147319064 + 4.493775893i
$TM_{112}$	8.806507980 + 0.898755178i	7.6268159739 + 4.493775893i
$TM_{112}$	8.806507980 + 0.898755178i	7.6268159739 + 4.493775893i
$TE_{011}$	6.622028662 + 0.898755178i	4.9462109435 + 4.493775893i
$TE_{011}$	6.622028662 + 0.898755178i	4.9462109435 + 4.493775893i
$TE_{012}$	8.806507980 + 0.898755178i	7.6268159739 + 4.493775893i
$TE_{012}$	8.806507980 + 0.898755178i	7.6268159739 + 4.493775893i
$TM_{012}$	7.569401941 + 0.898755178i	6.1570759982 + 4.493775893i
$TM_{012}$	7.569401941 + 0.898755178i	6.1570759982 + 4.493775893i
$TE_{111}$	4.259597004 + 0.898755178i	3.3792830626i
$TE_{111}$	4.259597004 + 0.898755178i	5.6082687247i
$TE_{121}$	8.668139654 + 0.898755178i	7.4666179868 + 4.493775893i
$TE_{121}$	8.668139654 + 0.898755178i	7.4666179868 + 4.493775893i
$TE_{211}$	5.627022570 + 0.898755178i	3.5038724429 + 4.493775893i
$TE_{211}$	5.627022570 + 0.898755178i	3.5038724429 + 4.493775893i
$TE_{112}$	7.200519831 + 0.898755178i	5.6974753121 + 4.493775893i
$TE_{112}$	7.200519831 + 0.898755178i	5.6974753121 + 4.493775893i
$TE_{311}$	7.113942250 + 0.898755178i	5.5876572403 + 4.493775893i
$TE_{311}$	7.113942250 + 0.898755178i	5.5876572403 + 4.493775893i
$TE_{212}$	8.084967669 + 0.898755178i	6.7808879432 + 4.493775893i
$TE_{212}$	8.084967669 + 0.898755178i	6.7808879432 + 4.493775893i
$TE_{411}$	8.648694425 + 0.898755178i	7.4440348174 + 4.493775893i
$TE_{411}$	8.648694425 + 0.898755178i	7.4440348174 + 4.493775893i



$\sigma$	10	50	100
$TM_{011}$	1.479169824i	0.272314901i	0.135847573i
$TM_{011}$	16.495933750i	89.603202971i	179.6151881i
$TM_{021}$	9.401774149i	88.969539179i	179.301488408i
$TM_{021}$	7.772418232 + 4.493775893i	8.573329425i	0.449547338i
$TM_{010}$	0.765007203i	0.146729359i	0.073274776i
$TM_{010}$	17.210096371i	89.728788513i	179.677760971i
$TM_{020}$	5.610271831i	0.778591020i	0.386755194i
$TM_{020}$	12.364831743i	89.096926852i	179.3642805i
$TM_{110}$	2.1063089937i	0.373450420i	0.186142090i
$TM_{110}$	15.868794580i	89.502067452i	179.5648936i
$TM_{210}$	13.540829209i	89.202399751i	179.4163742i
$TM_{210}$	4.434274365i	0.673118122i	0.334661493i
$TM_{310}$	8.513356451 + 4.493775893i	3.448937911 + 8.987551787i	0.517040641i
$TM_{310}$	3.448937911 + 8.987551787i	88.8323020876i	179.233995105i
$TM_{111}$	14.997299090i	89.375841183i	179.062539585i
$TM_{111}$	2.977804484i	0.499676689i	0.248793686i
$TM_{211}$	5.905686192i	0.800201384i	0.397417080i
$TM_{211}$	12.069417382i	89.075316489i	179.353618666i
$TM_{112}$	10.541174472i	88.994992560i	179.314023951i
$TM_{112}$	7.433929102i	0.880525313i	0.437011796i
$TE_{011}$	14.99729909i	89.375841183i	179.062539585i
$TE_{011}$	2.977804484i	0.499676689i	0.248793686i
$TE_{012}$	10.541174472i	88.994992560i	179.314023951i
$TE_{012}$	7.433929102i	0.880525313i	0.437011796i
$TM_{012}$	13.74911460i	89.224309622i	179.427207452i
$TM_{012}$	4.225988966i	0.651208251i	0.323828294i
$TE_{111}$	1.124717716i	0.211365713i	0.105496231i
$TE_{111}$	16.85038585i	89.664152160i	179.645539515i
$TE_{121}$	11.185660334i	89.022424891i	179.327540249i
$TE_{121}$	6.789443239i	0.853092982i	0.423495497i
$TE_{211}$	2.037376016i	0.362754344i	0.180827009i
$TE_{211}$	15.93772755i	89.512763528i	179.570208737i
$TE_{112}$	14.29046046i	89.285779541i	179.457622483i
$TE_{112}$	3.684643112i	0.589738332i	0.293413263i
$TE_{311}$	3.569050895i	0.575767964i	0.286496348i
$TE_{311}$	0.648388316i	0.125174336i	0.062521746i
$TE_{212}$	5.166344641i	0.742423038i	0.368902196i
$TE_{212}$	12.808758932i	89.133094835i	179.382133550i
$TE_{411}$	11.260965736i	89.0262438520i	179.329422410i
$TE_{411}$	6.7141378379i	0.849274021i	0.421613336i

Table 5: The Q factor of the homogeneous resonator as a function of conductivity.

$\sigma$	0.01	0.05	0.1	0.5	1	5	10	50	100
$TM_{011}$	274.805	54.959	27.476	5.473	2.702	0.228	0.000	0	0
$TM_{011}$	274.805	54.959	27.476	5.473	2.702	0.228	0.000	0	0
$TM_{021}$	499.468	99.892	49.944	9.977	4.970	0.865	0.000	0	0
$TM_{021}$	499.468	99.892	49.944	9.977	4.970	0.865	0.000	0	0
$TM_{010}$	201.861	40.369	20.180	4.006	1.956	0.000	0.000	0	0
$TM_{010}$	201.861	40.369	20.180	4.006	1.956	0.000	0.000	0	0
$TM_{020}$	463.356	92.670	46.333	9.254	4.607	0.780	0.000	0	0
$TM_{020}$	463.356	92.670	46.333	9.254	4.607	0.780	0.000	0	0
$TM_{110}$	321.633	64.325	32.159	6.413	3.177	0.405	0.000	0	0
$TM_{110}$	321.633	64.325	32.159	6.413	3.177	0.405	0.000	0	0
$TM_{210}$	431.084	86.215	43.106	8.607	4.282	0.702	0.000	0	0
$TM_{210}$	431.084	86.215	43.106	8.607	4.282	0.702	0.000	0	0
$TM_{310}$	535.551	107.109	53.553	10.699	5.332	0.947	0.192	0	0
$TM_{310}$	535.551	107.109	53.553	10.699	5.332	0.947	0.192	0	0
$TM_{111}$	371.777	74.354	37.174	7.419	3.684	0.550	0.000	0	0
$TM_{111}$	371.777	74.354	37.174	7.419	3.684	0.550	0.000	0	0
$TM_{211}$	469.685	93.936	46.966	9.380	4.670	0.795	0.000	0	0
$TM_{211}$	469.685	93.936	46.966	9.380	4.670	0.795	0.000	0	0
$TM_{112}$	492.473	98.493	49.245	9.837	4.899	0.849	0.000	0	0
$TM_{112}$	492.473	98.493	49.245	9.837	4.899	0.849	0.000	0	0
$TE_{011}$	371.777	74.354	37.174	7.419	3.684	0.550	0.000	0	0
$TE_{011}$	371.777	74.354	37.174	7.419	3.684	0.550	0.000	0	0
$TE_{012}$	492.473	98.493	49.245	9.837	4.899	0.849	0.000	0	0
$TE_{012}$	492.473	98.493	49.245	9.837	4.899	0.849	0.000	0	0
$TM_{012}$	424.062	84.811	42.403	8.467	4.211	0.685	0.000	0	0
$TM_{012}$	424.062	84.811	42.403	8.467	4.211	0.685	0.000	0	0
$TE_{111}$	242.189	48.435	24.214	4.818	2.370	0.000	0.000	0	0
$TE_{111}$	242.189	48.435	24.214	4.818	2.370	0.000	0.000	0	0
$TE_{121}$	484.815	96.962	48.479	9.683	4.822	0.831	0.000	0	0
$TE_{121}$	484.815	96.962	48.479	9.683	4.822	0.831	0.000	0	0
$TE_{211}$	317.013	63.401	31.697	6.321	3.130	0.390	0.000	0	0
$TE_{211}$	317.013	63.401	31.697	6.321	3.130	0.390	0.000	0	0
$TE_{112}$	403.691	80.737	40.366	8.058	4.006	0.634	0.000	0	0
$TE_{112}$	403.691	80.737	40.366	8.058	4.006	0.634	0.000	0	0
$TE_{311}$	398.912	79.781	39.888	7.963	3.958	0.622	0.000	0	0
$TE_{311}$	398.912	79.781	39.888	7.963	3.958	0.622	0.000	0	0
$TE_{212}$	452.557	90.510	45.253	9.037	4.498	0.754	0.000	0	0
$TE_{212}$	452.557	90.510	45.253	9.037	4.498	0.754	0.000	0	0
$TE_{411}$	483.739	96.747	48.371	9.662	4.811	0.828	0.000	0	0
$TE_{411}$	483.739	96.747	48.371	9.662	4.811	0.828	0.000	0	0

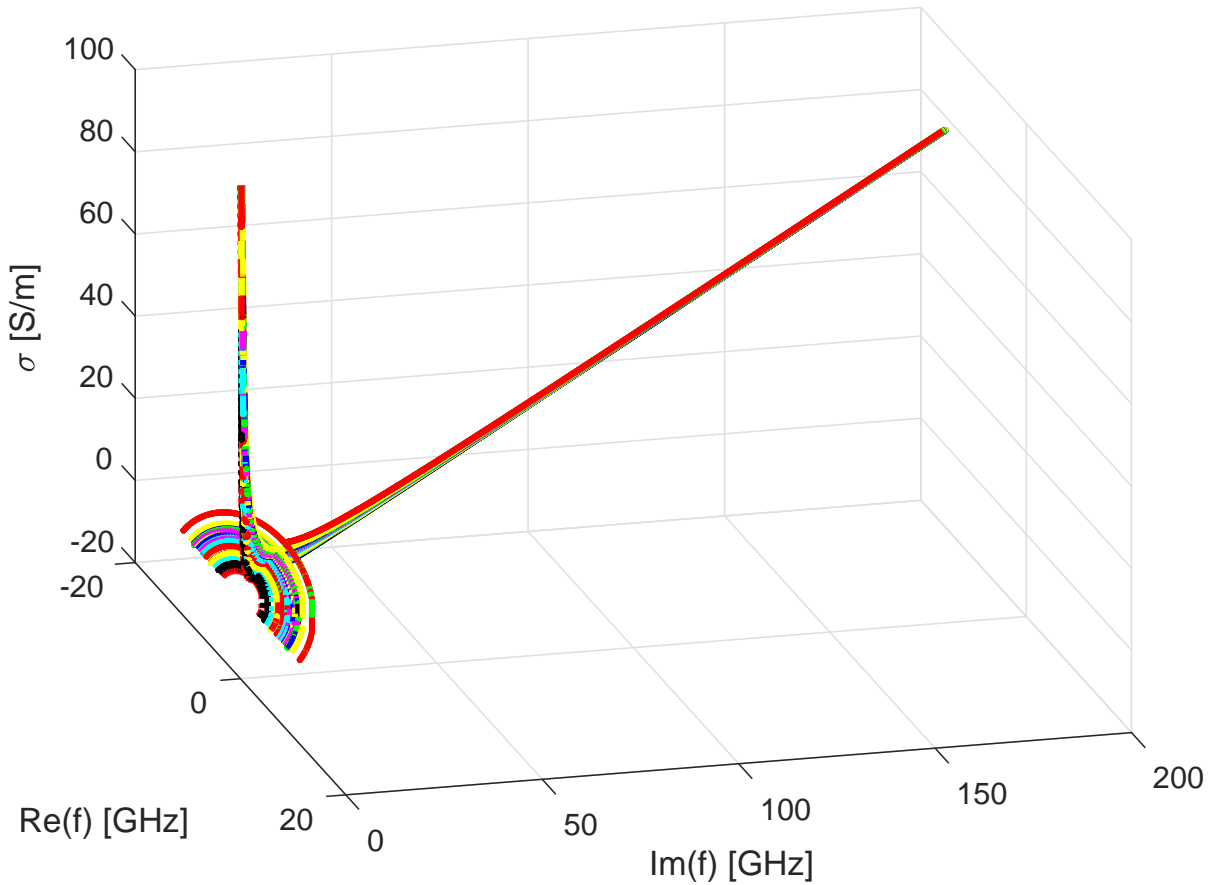


Figure 2: The complex resonance frequencies for a homogeneous cylindrical resonator as a function of conductivity (legend in table 1).

## 4 Summary

The global root finding algorithm is proven to be very useful in the analysis of the structures filled with lossy material. Finding roots is very efficient. Results of the analysis were confirmed by checking the transition between  $\epsilon_{r2} = 10$  and  $\epsilon_{r2} = 1$  and between lossy material (high value of  $\sigma$ ) and perfect electric conductor.

## References

- [1] P. Kowalczyk, "Complex Root Finding Algorithm Based on Delaunay Triangulation", *ACM Trans. Math. Softw.*, vol. 41,no. 3, pp. 19:1-19:13, Jun. 2015.

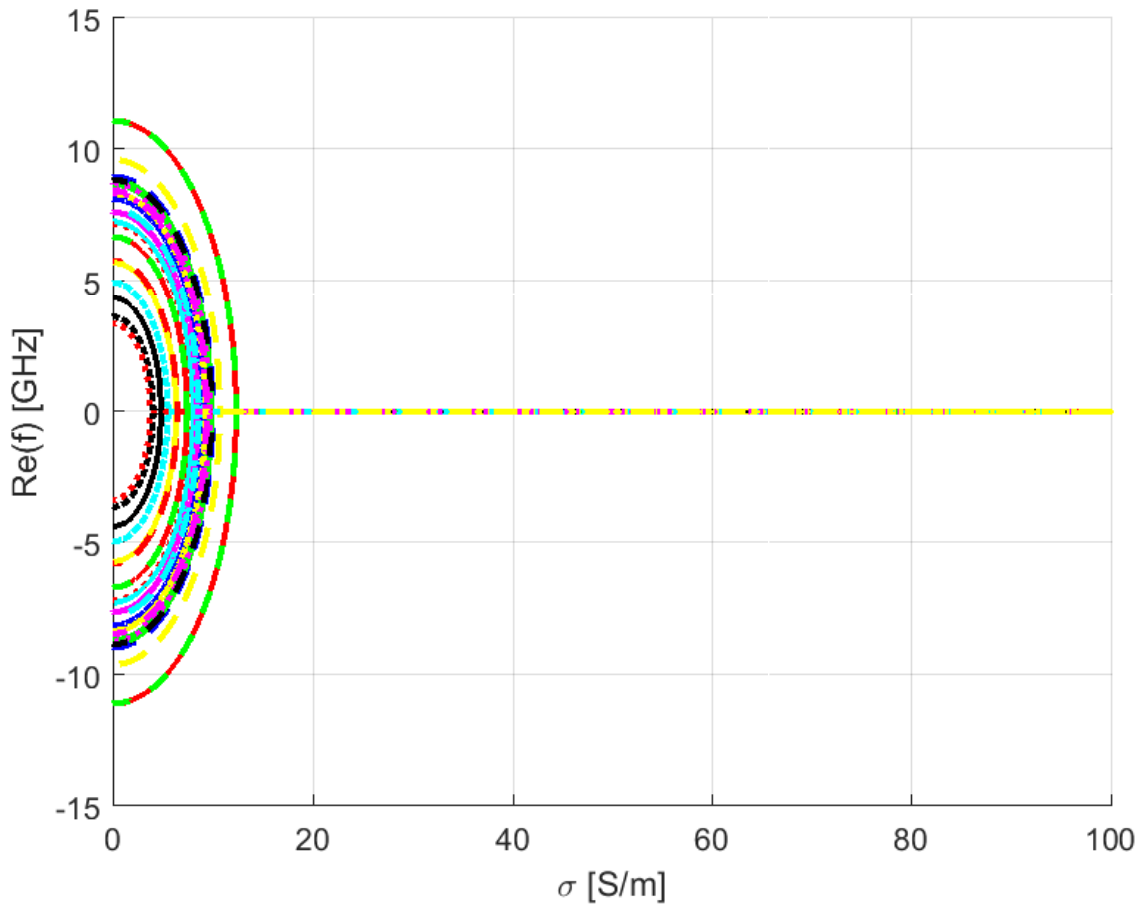


Figure 3: The real part of the resonance frequencies for a homogeneous cylindrical resonator as a function of conductivity (legend in table 1).

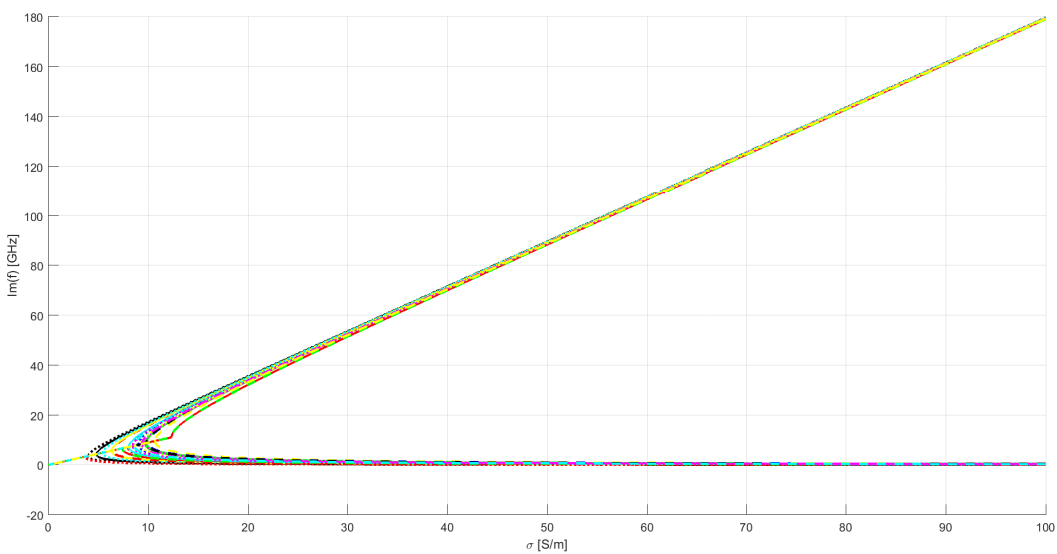


Figure 4: The imaginary part of the resonance frequencies for a homogeneous cylindrical resonator as a function of losses (legend in table 1).

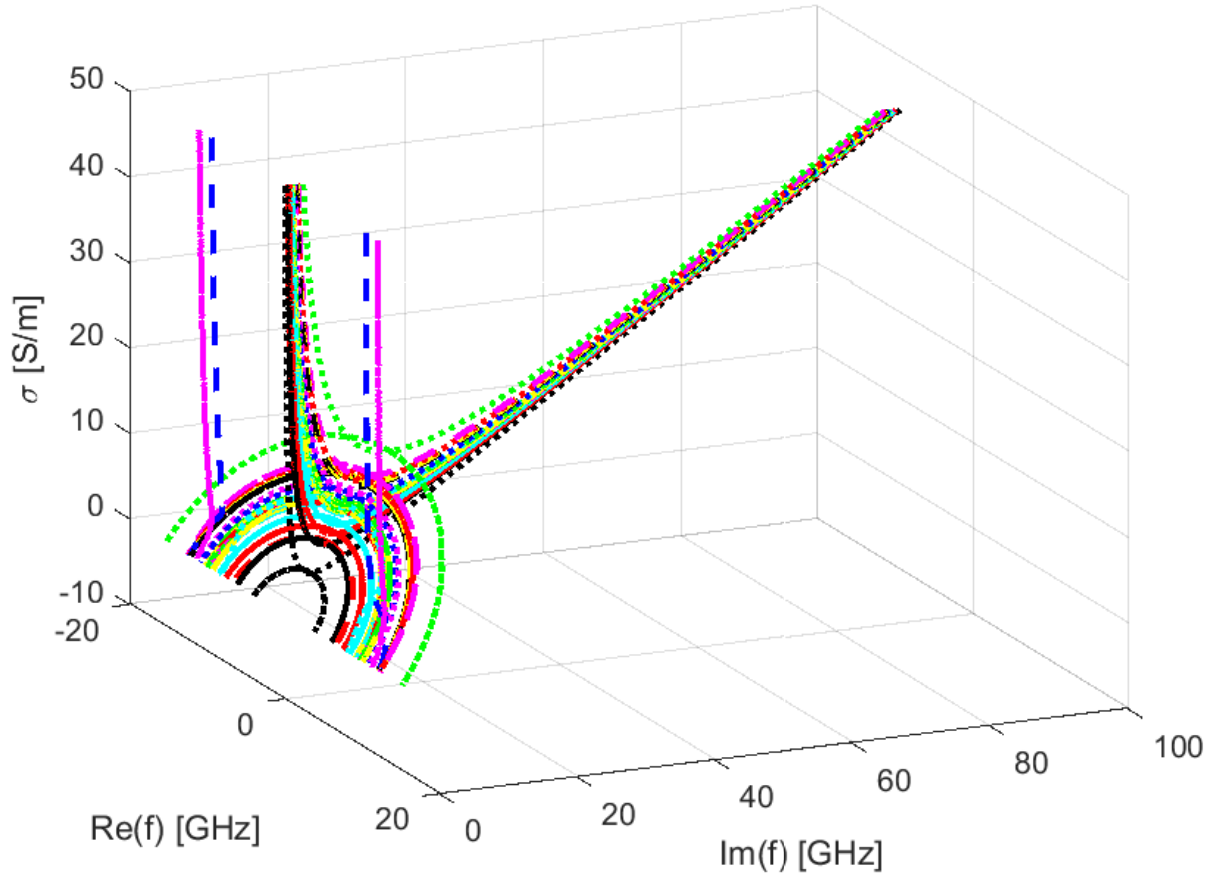


Figure 5: The complex resonance frequencies for a coaxially loaded cylindrical resonator as a function of losses (A legend in the table 5).

Table 6: Modes presented in the Fig.5-7.

mode	color in a figure	line style
$HE_{011}$	red	solid
$HE_{012}$	green	solid
$HE_{111}$	black	solid
$HE_{112}$	cyan	solid
$HE_{121}$	magenta	solid
$HE_{211}$	yellow	solid
$HE_{212}$	blue	dotted
$HE_{311}$	red	dotted
$HE_{411}$	green	dotted
$TM_{010}$	black	dotted
$TM_{011}$	cyan	dotted
$TM_{012}$	magenta	dotted
$TM_{020}$	yellow	dotted
$TM_{021}$	blue	dashed
$TM_{110}$	red	dashed
$EH_{111}$	green	dashed
$EH_{112}$	black	dashed
$TM_{210}$	cyan	dashed
$EH_{211}$	magenta	dashed
$TM_{310}$	yellow	dashed

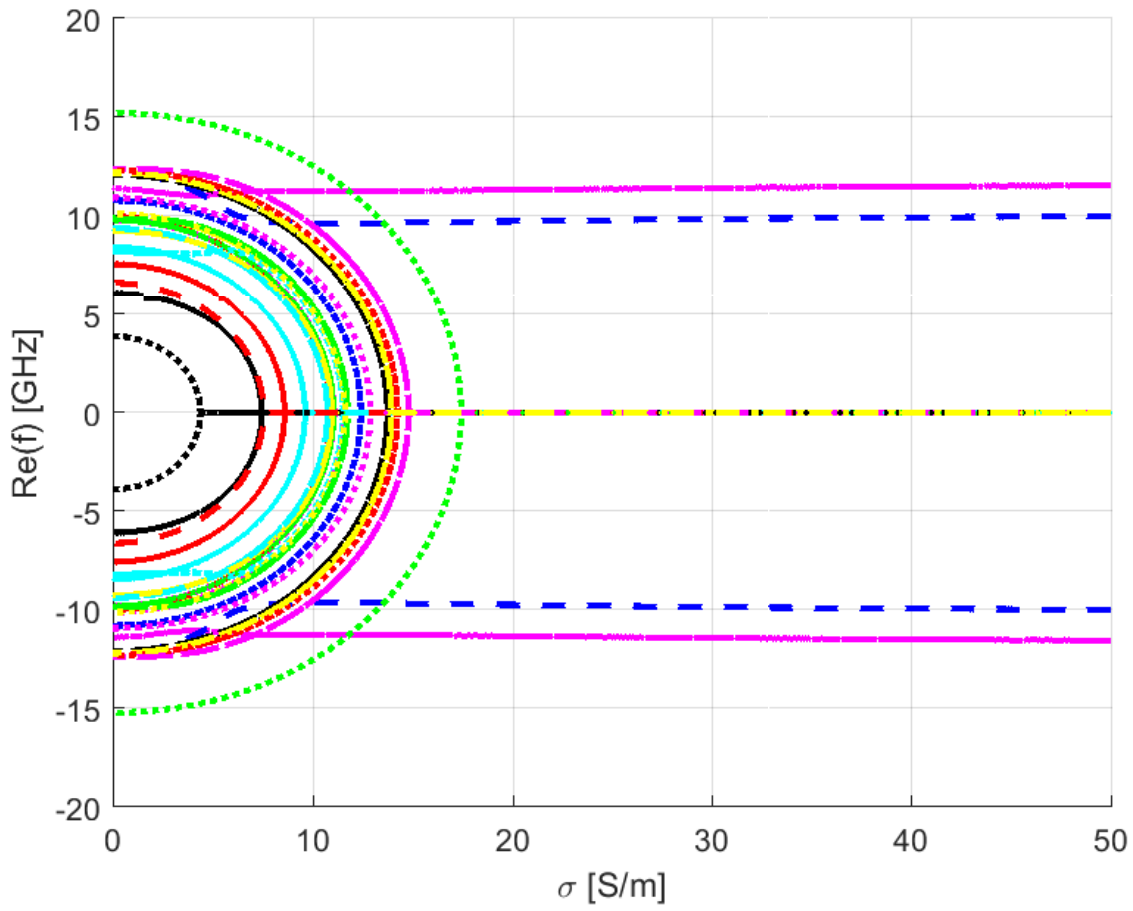


Figure 6: The real part of the resonance frequencies for a coaxially loaded cylindrical resonator as a function of conductivity (legend in table 5).

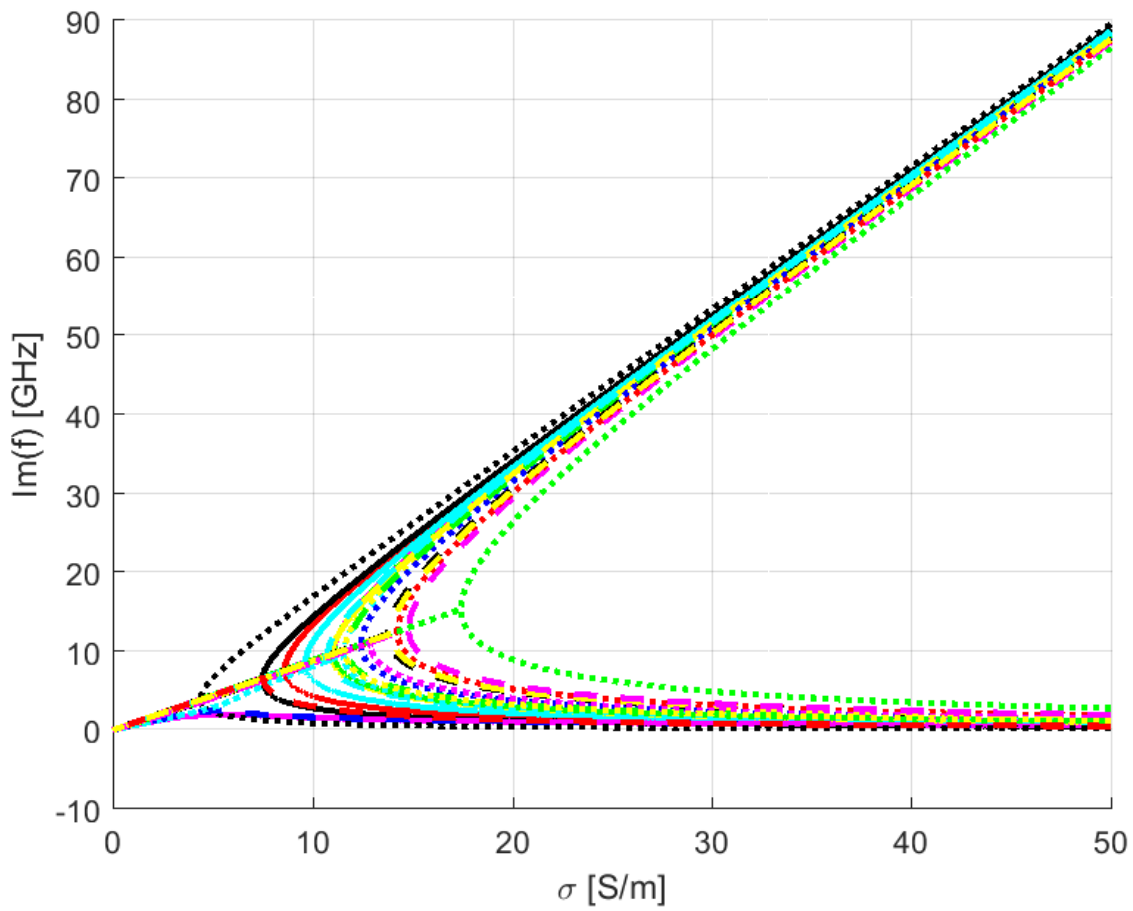


Figure 7: The imaginary part of the resonance frequencies for a coaxially loaded cylindrical resonator as a function of conductivity (legend in table 5).

Table 7: The resonance frequencies of the coaxially loaded resonator as a function of conductivity.

$\sigma$	0.01	0.05
$TM_{011}$	8.193371311 + 0.005620955i	8.193334914 + 0.028104559i
$TM_{011}$	8.193371311 + 0.005620955i	8.193334914 + 0.028104559i
$TM_{021}$	12.187611798 + 0.005710941i	12.187494894 + 0.028554449i
$TM_{010}$	3.883846836 + 0.008860728i	3.883604478 + 0.044303647i
$TM_{010}$	3.883846836 + 0.008860728i	3.883604478 + 0.044303647i
$TM_{020}$	10.120289968 + 0.008680030i	10.120201536 + 0.043400162i
$TM_{020}$	10.120289968 + 0.008680030i	10.120201536 + 0.043400162i
$TM_{110}$	6.618760142 + 0.008760717i	6.618621574 + 0.043803594i
$TM_{110}$	6.618760142 + 0.008760717i	6.618621574 + 0.043803594i
$TM_{210}$	9.389882430 + 0.008708655i	9.389786361 + 0.043543286i
$TM_{210}$	9.389882430 + 0.008708655i	9.389786361 + 0.043543286i
$TM_{310}$	12.204093597 + 0.008698429i	12.204020158 + 0.043492153i
$TM_{310}$	12.204093597 + 0.008698429i	12.204020158 + 0.043492153i
$EH_{111}$	9.884742887 + 0.007439087i	9.884725417 + 0.037195934i
$EH_{111}$	9.884742887 + 0.007439087i	9.884725417 + 0.037195934i
$EH_{211}$	12.403655641 + 0.007566035i	12.403630797 + 0.037830449i
$EH_{211}$	12.403655641 + 0.007566035i	12.403630797 + 0.037830449i
$EH_{112}$	12.101983726 + 0.008754416i	12.101909095 + 0.043772094i
$EH_{112}$	12.101983726 + 0.008754416i	12.101909095 + 0.043772094i
$HE_{011}$	7.575021632 + 0.008797067i	7.574899551 + 0.043985342i
$HE_{011}$	7.575021632 + 0.008797067i	7.574899551 + 0.043985342i
$HE_{012}$	9.809556454 + 0.008865483i	9.809460643 + 0.044327420i
$HE_{012}$	9.809556454 + 0.008865483i	9.809460643 + 0.044327420i
$TM_{012}$	10.941787080 + 0.008321628i	10.941715211 + 0.041608179i
$TM_{012}$	10.941787080 + 0.008321628i	10.941715211 + 0.041608179i
$HE_{111}$	6.088970461 + 0.007932438i	6.088853781 + 0.039662276i
$HE_{111}$	6.088970461 + 0.007932438i	6.088853781 + 0.039662276i
$HE_{121}$	11.393801008 + 0.005813773i	11.393707068 + 0.029067930i
$HE_{211}$	9.258477841 + 0.008125147i	9.258404003 + 0.040625872i
$HE_{211}$	9.258477841 + 0.008125147i	9.258404003 + 0.040625872i
$HE_{112}$	8.439291092 + 0.008753105i	8.439182696 + 0.043765533i
$HE_{112}$	8.439291092 + 0.008753105i	8.439182696 + 0.043765533i
$HE_{311}$	12.308459456 + 0.008457335i	12.308395401 + 0.042286733i
$HE_{311}$	12.308459456 + 0.008457335i	12.308395401 + 0.042286733i
$HE_{212}$	10.796262626 + 0.008632330i	10.796181356 + 0.043161666i
$HE_{212}$	10.796262626 + 0.008632330i	10.796181356 + 0.043161666i
$HE_{411}$	15.220917038 + 0.008627365i	15.220860786 + 0.043136845i
$HE_{411}$	15.220917038 + 0.008627365i	15.220860786 + 0.043136845i



$\sigma$	0.1	0.5
$TM_{011}$	8.193221216 + 0.056207766i	8.189615971 + 0.280824146i
$TM_{011}$	8.193221216 + 0.056207766i	8.189615971 + 0.280824146i
$TM_{021}$	12.187129551 + 0.057107300i	12.175423561 + 0.285279855i
$TM_{010}$	3.882847010 + 0.088607329i	3.858528887 + 0.443041996i
$TM_{010}$	3.882847010 + 0.088607329i	3.858528887 + 0.443041996i
$TM_{020}$	10.119925179 + 0.086800376i	10.111077389 + 0.434010120i
$TM_{020}$	10.119925179 + 0.086800376i	10.111077389 + 0.434010120i
$TM_{110}$	6.618188531 + 0.087607238i	6.604315581 + 0.438044227i
$TM_{110}$	6.618188531 + 0.087607238i	6.604315581 + 0.438044227i
$TM_{210}$	9.389486139 + 0.087086625i	9.379873518 + 0.435441592i
$TM_{210}$	9.389486139 + 0.087086625i	9.379873518 + 0.435441592i
$TM_{310}$	12.203790657 + 0.086984354i	12.196444018 + 0.434929288i
$TM_{310}$	12.203790657 + 0.086984354i	12.196444018 + 0.434929288i
$EH_{111}$	9.884670823 + 0.074394986i	9.882923195 + 0.372480214i
$EH_{111}$	9.884670823 + 0.074394986i	9.882923195 + 0.372480214i
$EH_{211}$	12.403553149 + 0.075662586i	12.401059710 + 0.378583721i
$EH_{211}$	12.403553149 + 0.075662586i	12.401059710 + 0.378583721i
$EH_{112}$	12.101675867 + 0.087544268i	12.094209449 + 0.437734208i
$EH_{112}$	12.101675867 + 0.087544268i	12.094209449 + 0.437734208i
$HE_{011}$	7.574518033 + 0.087970723i	7.562298922 + 0.439859883i
$HE_{011}$	7.574518033 + 0.087970723i	7.562298922 + 0.439859883i
$HE_{012}$	9.809161225 + 0.088654862i	9.799574879 + 0.443277548i
$HE_{012}$	9.809161225 + 0.088654862i	9.799574879 + 0.443277548i
$TM_{012}$	10.941490617 + 0.083216579i	10.934299533 + 0.416118267i
$TM_{012}$	10.941490617 + 0.083216579i	10.934299533 + 0.416118267i
$HE_{111}$	6.088489138 + 0.079325075i	6.076806431 + 0.396709619i
$HE_{111}$	6.088489138 + 0.079325075i	6.076806431 + 0.396709619i
$HE_{121}$	11.393413534 + 0.058129991i	11.384044884 + 0.289704562i
$HE_{211}$	9.258173247 + 0.081252596i	9.250776906 + 0.406398800i
$HE_{211}$	9.258173247 + 0.081252596i	9.250776906 + 0.406398800i
$HE_{112}$	8.438843948 + 0.087531104i	8.427996479 + 0.437661516i
$HE_{112}$	8.438843948 + 0.087531104i	8.427996479 + 0.437661516i
$HE_{311}$	12.308195224 + 0.084573822i	12.301784167 + 0.422925853i
$HE_{311}$	12.308195224 + 0.084573822i	12.301784167 + 0.422925853i
$HE_{212}$	10.795927385 + 0.086323420i	10.787796433 + 0.431631229i
$HE_{212}$	10.795927385 + 0.086323420i	10.787796433 + 0.431631229i
$HE_{411}$	15.220684998 + 0.086273812i	15.215057695 + 0.431388471i
$HE_{411}$	15.220684998 + 0.086273812i	15.215057695 + 0.431388471i

$\sigma$	1	5
$TM_{011}$	8.178765458 + 0.560345563i	8.184165712 + 2.848508919i
$TM_{011}$	8.178765458 + 0.560345563i	8.184165712 + 2.848508919i
$TM_{021}$	12.138652932 + 0.568935348i	10.767934432 + 2.425160251i
$TM_{010}$	3.781518960 + 0.886117318i	6.573751903i
$TM_{010}$	3.781518960 + 0.886117318i	2.297249665i
$TM_{020}$	10.083373120 + 0.868071630i	9.148529762 + 4.348229816i
$TM_{020}$	10.083373120 + 0.868071630i	9.148529762 + 4.348229816i
$TM_{110}$	6.560766410 + 0.876138529i	4.962572954 + 4.388177543i
$TM_{110}$	6.560766410 + 0.876138529i	4.962572954 + 4.388177543i
$TM_{210}$	9.349764862 + 0.870935955i	8.324340318 + 4.362636784i
$TM_{210}$	9.349764862 + 0.870935955i	8.324340318 + 4.362636784i
$TM_{310}$	12.173453232 + 0.869905450i	11.410108443 + 4.356642312i
$TM_{310}$	12.173453232 + 0.869905450i	11.410108443 + 4.356642312i
$EH_{111}$	9.877412788 + 0.748273488i	9.265427451 + 4.185444420i
$EH_{111}$	9.877412788 + 0.748273488i	9.265427451 + 4.185444420i
$EH_{211}$	12.393151818 + 0.758879422i	11.977818451 + 4.047516883i
$EH_{211}$	12.393151818 + 0.758879422i	11.977818451 + 4.047516883i
$EH_{112}$	12.070837710 + 0.875548084i	11.290976214 + 4.388175965i
$EH_{112}$	12.070837710 + 0.875548084i	11.290976214 + 4.388175965i
$HE_{011}$	7.523981348 + 0.879758825i	6.168967803 + 4.404652172i
$HE_{011}$	7.523981348 + 0.879758825i	6.168967803 + 4.404652172i
$HE_{012}$	9.769554869 + 0.886575287i	8.752996788 + 4.435934599i
$HE_{012}$	9.769554869 + 0.886575287i	8.752996788 + 4.435934599i
$TM_{012}$	10.911776377 + 0.832457045i	10.147887577 + 4.195155460i
$TM_{012}$	10.911776377 + 0.832457045i	10.147887577 + 4.195155460i
$HE_{111}$	6.040116668 + 0.793958918i	4.634133366 + 4.078281304i
$HE_{111}$	6.040116668 + 0.793958918i	4.634133366 + 4.078281304i
$HE_{121}$	11.355116244 + 0.573343701i	11.098814421 + 1.956280269i
$HE_{211}$	9.227511901 + 0.813638733i	8.367157908 + 4.172468014i
$HE_{211}$	9.227511901 + 0.813638733i	8.367157908 + 4.172468014i
$HE_{112}$	8.394003497 + 0.875360400i	7.218491308 + 4.382427531i
$HE_{112}$	8.394003497 + 0.875360400i	7.218491308 + 4.382427531i
$HE_{311}$	12.281682782 + 0.846202112i	11.590631439 + 4.273896444i
$HE_{311}$	12.281682782 + 0.846202112i	11.590631439 + 4.273896444i
$HE_{212}$	10.762338792 + 0.863350408i	9.906220907 + 4.329605914i
$HE_{212}$	10.762338792 + 0.863350408i	9.906220907 + 4.329605914i
$HE_{411}$	15.197446386 + 0.862897257i	14.614092918 + 4.330563863i
$HE_{411}$	15.197446386 + 0.862897257i	14.614092918 + 4.330563863i

$\sigma$	10	50
$TM_{011}$	5.013125671 + 8.082320397i	1.062711507i
$TM_{011}$	5.013125671 + 8.082320397i	88.094642316i
$TM_{021}$	9.658158439 + 1.632617845i	10.001361011 + 0.657079908i
$TM_{010}$	16.891374321i	89.564677852i
$TM_{010}$	0.8963027467i	0.1705263881i
$TM_{020}$	5.168290966 + 8.737693702i	1.193490361i
$TM_{020}$	5.168290966 + 8.737693702i	88.204459867i
$TM_{110}$	3.015641971i	0.502423287i
$TM_{110}$	14.609775671i	88.328269708i
$TM_{210}$	3.446264103 + 8.765105550i	88.433098749i
$TM_{210}$	3.446264103 + 8.765105550i	1.022317464i
$TM_{310}$	8.554474315 + 8.749768882i	87.621308430i
$TM_{310}$	8.554474315 + 8.749768882i	1.741975509i
$EH_{111}$	5.416164437 + 8.681022277i	88.198129721i
$EH_{111}$	5.416164437 + 8.681022277i	1.211258954i
$EH_{211}$	9.533642567 + 8.538014300i	1.929323611i
$EH_{211}$	9.533642567 + 8.538014300i	87.286222675i
$EH_{112}$	8.340528937 + 8.814170236i	87.805392675i
$EH_{112}$	8.340528937 + 8.814170236i	1.699975331i
$HE_{011}$	13.363176911i	88.952455487i
$HE_{011}$	4.313059812i	0.656512797i
$HE_{012}$	4.179020621 + 8.887452320i	1.098108685i
$HE_{012}$	4.179020621 + 8.887452320i	88.566013094i
$TM_{012}$	7.034355376 + 8.536163719i	1.446938383i
$TM_{012}$	7.034355376 + 8.536163719i	88.566013094i
$HE_{111}$	14.303944181i	88.973277409i
$HE_{111}$	2.769965631i	0.462997396i
$HE_{121}$	11.267428118 + 1.567485972i	11.556368348 + 0.632450871i
$HE_{211}$	3.918216906 + 8.599795786i	88.323651569i
$HE_{211}$	3.918216906 + 8.599795786i	1.042072260i
$HE_{112}$	11.19953032i	88.650592994i
$HE_{112}$	6.387075514i	0.820378611i
$HE_{311}$	8.886854012 + 8.669948369i	87.509117912i
$HE_{311}$	8.886854012 + 8.669948369i	1.804362029i
$HE_{212}$	6.448047153 + 8.717360493i	87.992859637i
$HE_{212}$	6.448047153 + 8.717360493i	1.366178046i
$HE_{411}$	12.548575679 + 8.720663650i	2.752193243i
$HE_{411}$	12.548575679 + 8.720663650i	86.522940987i

Table 8: The Q factor of the coaxially loaded resonator as a function of conductivity.

$\sigma$	0.01	0.05	0.1	0.5	1	5	10	50
$TM_{011}$	728.824	145.765	72.883	14.581	7.298	1.437	0.310	0.000
$TM_{011}$	728.824	145.765	72.883	14.581	7.298	1.437	0.310	0.000
$TM_{021}$	1067.041	213.408	106.704	21.339	10.668	2.220	2.958	7.610
$TM_{010}$	219.161	43.829	21.910	4.355	2.134	0.000	0.000	0.000
$TM_{010}$	219.161	43.829	21.910	4.355	2.134	0.000	0.000	0.000
$TM_{020}$	582.964	116.592	58.294	11.648	5.808	1.052	0.296	0.000
$TM_{020}$	582.964	116.592	58.294	11.648	5.808	1.052	0.296	0.000
$TM_{110}$	377.752	75.549	37.772	7.538	3.744	0.565	0.000	0.000
$TM_{110}$	377.752	75.549	37.772	7.538	3.744	0.565	0.000	0.000
$TM_{210}$	539.112	107.821	53.909	10.771	5.368	0.954	0.197	0.000
$TM_{210}$	539.112	107.821	53.909	10.771	5.368	0.954	0.197	0.000
$TM_{310}$	701.511	140.301	70.149	14.021	6.997	1.310	0.489	0.000
$TM_{310}$	701.511	140.301	70.149	14.021	6.997	1.310	0.489	0.000
$EH_{111}$	664.379	132.874	66.434	13.266	6.600	1.107	0.312	0.000
$EH_{111}$	664.379	132.874	66.434	13.266	6.600	1.107	0.312	0.000
$EH_{211}$	819.693	163.937	81.966	16.378	8.165	1.480	0.558	0.000
$EH_{211}$	819.693	163.937	81.966	16.378	8.165	1.480	0.558	0.000
$EH_{112}$	691.193	138.238	69.117	13.815	6.893	1.287	0.473	0.000
$EH_{112}$	691.193	138.238	69.117	13.815	6.893	1.287	0.473	0.000
$HE_{011}$	430.542	86.107	43.051	8.596	4.276	0.700	0.000	0.000
$HE_{011}$	430.542	86.107	43.051	8.596	4.276	0.700	0.000	0.000
$HE_{012}$	553.244	110.648	55.322	11.054	5.510	0.987	0.235	0.000
$HE_{012}$	553.244	110.648	55.322	11.054	5.510	0.987	0.235	0.000
$TM_{012}$	657.431	131.485	65.741	13.138	6.554	1.209	0.412	0.000
$TM_{012}$	657.431	131.485	65.741	13.138	6.554	1.209	0.412	0.000
$HE_{111}$	383.802	76.759	38.377	7.659	3.804	0.568	0.000	0.000
$HE_{111}$	383.802	76.759	38.377	7.659	3.804	0.568	0.000	0.000
$HE_{121}$	979.897	195.984	97.999	19.648	9.903	2.837	3.594	9.136
$HE_{211}$	569.742	113.947	56.972	11.381	5.671	1.003	0.228	0.000
$HE_{211}$	569.742	113.947	56.972	11.381	5.671	1.003	0.228	0.000
$HE_{112}$	482.074	96.414	48.205	9.628	4.795	0.824	0.000	0.000
$HE_{112}$	482.074	96.414	48.205	9.628	4.795	0.824	0.000	0.000
$HE_{311}$	727.680	145.535	72.766	14.544	7.257	1.356	0.513	0.000
$HE_{311}$	727.680	145.535	72.766	14.544	7.257	1.356	0.513	0.000
$HE_{212}$	625.339	125.067	62.532	12.497	6.233	1.144	0.370	0.000
$HE_{212}$	625.339	125.067	62.532	12.497	6.233	1.144	0.370	0.000
$HE_{411}$	882.130	176.425	88.212	17.635	8.806	1.687	0.719	0.000
$HE_{411}$	882.130	176.425	88.212	17.635	8.806	1.687	0.719	0.000

Table 9: The resonance frequencies of the coaxially loaded with perfect electric conductor resonator .

mode	$TM_{021}$	$HE_{121}$
$\sigma = 50$	10.001361011 + 0.657079908i	11.556368348 + 0.632450871i
$\sigma = 100$	10.163284506 + 0.455216508i	11.707184913 + 0.436944723i
$\sigma = 500$	10.399584353 + 0.200637890i	11.931322113 + 0.192012576i
$\sigma \rightarrow \infty$	10.599264000	12.122082950
mode	$TEM_1$	$TE_{111}$